# The Auxin *Sl-IAA17* Transcriptional Repressor Controls Fruit Size Via the Regulation of Endoreduplication-Related Cell Expansion

Liyan Su[1,2], Carole Bassa[1,2], Corinne Audran[1,2], Isabelle Mila[1,2], Catherine Cheniclet[3,4], Christian Chevalier[3,4], Mondher Bouzayen[1,2], Jean-Paul Roustan[1,2] and Christian Chervin[1,2,*]

[1]Université de Toulouse, INP-ENSA Toulouse, UMR990 Génomique et Biotechnologie des Fruits, Avenue de l'Agrobiopole, CS 32607, F-31326 Castanet-Tolosan, France
[2]INRA, UMR990 Génomique et Biotechnologie des Fruits, 24 Chemin de Borde Rouge, CS 52627, F-31326 Castanet-Tolosan, France
[3]INRA, UMR1332 Biologie du Fruit et Pathologie, CS 20032, F-33882 Villenave d'Ornon, France
[4]Université de Bordeaux, UMR1332 Biologie du Fruit et Pathologie, INRA, CS 20032, F-33882 Villenave d'Ornon, France
*Corresponding author. E-mail, chervin@ensat.fr; Fax, +33-534-323-873.

**Auxin is known to regulate cell division and cell elongation, thus controlling plant growth and development. Part of the auxin signaling pathway depends on the fine-tuned degradation of the auxin/indole acetic acid (Aux/IAA) transcriptional repressors. Recent evidence indicates that Aux/IAA proteins play a role in fruit development in tomato (*Solanum lycopersicum* Mill.), a model species for fleshy fruit development. We report here on the functional characterization of *Sl-IAA17* during tomato fruit development. Silencing of *Sl-IAA17* by an RNA interference (RNAi) strategy resulted in the production of larger fruit than the wild type. Histological analyses of the fruit organ and tissues demonstrated that this phenotype was associated with a thicker pericarp, rather than larger locules and/or a larger number of seeds. Microscopic analysis demonstrated that the higher pericarp thickness in *Sl-IAA17* RNAi fruits was not due to a larger number of cells, but to the increase in cell size. Finally, we observed that the cell expansion in the transgenic fruits is tightly coupled with higher ploidy levels than in the wild type, suggesting a stimulation of the endoreduplication process. In conclusion, this work provides new insights into the function of the Aux/IAA pathway in fleshy fruit development, especially fruit size and cell size determination in tomato.**

**Keywords:** Aux/IAA • Auxin • Cell expansion • Endoreduplication • Fruit development • Tomato.

**Abbrevations:** ARF, auxin response factor; Aux/IAA, auxin/indole acetic acid; CaMV, *Cauliflower mosaic virus*; dpa, days post-anthesis; EI, endoreplication index; MS, Murashige and Skoog; NLS, nuclear localization signal; qRT–PCR, quantitative reverse transcription–PCR; RNAi, RNA interference; Sl-IAA, *Solanum lycopersicum* auxin/IAA; TIR1, transport inhibitor response1; YFP, yellow fluorescent protein.

## Introduction

Auxin is greatly involved in all stages of fruit development (Pattison et al. 2014, and references therein). A recent study has highlighted some of its roles in controlling fruit size in apple (Devoghalaere et al. 2012). In tomato, the final fruit size is largely influenced by cell expansion which itself is dependent upon endopolyploidy occurring via the endoreduplication process (Cheniclet et al. 2005). Indeed, modifying endoreduplication during fruit development greatly impacts fruit growth and final fruit size (for a review, see Chevalier et al. 2014). In Arabidopsis tissues, the link between endopolyploidy and auxin has been established by Ishida et al. (2010) demonstrating that low levels of the auxin signaling complex lead to increased endopolyploidy. However, the link between tomato fruit size, endopolyploidy and auxin is yet to be shown.

Understanding of the molecular mechanisms of auxin metabolism and perception is now well advanced in the model plant Arabidopsis, as reviewed by Ljung (2013) and Bargmann and Estelle (2014). As regards the signaling level, auxin promotes the degradation of auxin/indole acetic acid (Aux/IAA) proteins by stimulating their interaction with the $SCF^{TIR1}$ E3 ubiquitin ligase complex, where transport inhibitor response1 (TIR1) acts as the auxin receptor (Dharmasiri et al. 2005, Kepinski and Leyser 2005). The 26S proteasome degrades the ubiquitinylated Aux/IAA transcriptional repressors, allowing auxin-responsive factors (ARFs) to regulate the expression of their target genes. In recent years, building on the determination of the whole genome sequence (Tomato Genome Consortium. 2012), the complete set of *Aux/IAA* and *ARF* genes has been isolated in tomato, a model plant for both Solanaceae and fleshy fruit species, thus laying the ground for functional characterization and spatio-temporal expression studies of the two gene family members (Audran-Delalande et al. 2012, Hao et al. 2014, Zouine et al. 2014). Furthermore, the physiological significance of several Aux/IAA and ARF proteins has been addressed through reverse genetics approaches demonstrating their participation in the control of fruit development in tomato, such as Sl-IAA9 (Wang et al. 2005), Sl-IAA27 (Bassa et al. 2012), Sl-ARF4 (Sagar et al. 2013, and references therein), Sl-ARF7 (De Jong et al. 2009) and an ortholog of AtARF8 (Goetz et al. 2006).

The present study aimed at unraveling the function of *Sl-IAA17*, a member of the Aux/IAA multigene family, during tomato fruit development. The identification of gain-of-function mutations in the cluster of Aux/IAA genes closely related to *Sl-IAA17* in Arabidopsis (*IAA16*, *IAA7/AXR2*, *IAA14/SLR* and *IAA17/AXR3*) suggested that these proteins play important roles in inhibiting auxin responses in a variety of tissues and developmental programs (Rinaldi et al. 2012). Previous studies showed that *Sl-IAA17*-encoded proteins function as active repressors of auxin-dependent gene transcription (Audran-Delalande et al. 2012). On the other hand, the suppression of a closely related *Sl-IAA17* gene in potato, *St-IAA2*, resulted in clear phenotypes including increased plant height, petiole hyponasty and curvature of growing leaf primordia in the shoot apex without affecting tuber formation (Kloosterman et al. 2006). To address the potential role of *Sl-IAA17* in fruit development, RNA interference (RNAi) transgenic lines were generated, resulting in the down-regulation of the *Sl-IAA17* gene in tomato fruits. Fruit phenotyping and histological analyses of fruit tissues revealed the involvement of this Aux/IAA in the control of fruit size and ploidy levels.

## Results

### Sl-IAA17, a canonical Aux/IAA protein, is exclusively localized within the nucleus

*Sl-IAA17* has been identified previously as a member of the tomato *Aux/IAA* gene family which encompasses 25 members in tomato (Audran-Delalande et al. 2012). The phylogenetic analysis between Arabidopsis and tomato Aux/IAAs showed that *Sl-IAA17* and its closest tomato homologs *Sl-IAA7*, *Sl-IAA14* and *Sl-IAA16*, together with their closest Arabidopsis homologs *At-IAA17*, *At-IAA7*, *At-IAA14* and *At-IAA16*, belong to a distinct clade, named clade C (Audran-Delalande et al. 2012). The *Sl-IAA17* open reading frame is 627 bp long encoding a putative protein of 209 amino acids. Sl-IAA17 harbors the four conserved amino acid sequence motifs known as domains I, II, III and IV found in Aux/IAA proteins (**Supplementary Fig. S1**). As a common characteristics of clade C members, Sl-IAA17 contains a second putative repressor domain (DLxLxL) in the close vicinity of repression domain I. Like the majority of Aux/IAA proteins, Sl-IAA17 displays two conserved nuclear localization signal (NLS) domains: a bipartite structure of a conserved basic doublet KR between domains I and II associated with basic amino acids in domain II, and the SV40-type NLS located in domain IV (**Supplementary Fig. S1**). To analyze its subcellular localization, a translational fusion between Sl-IAA17 and the yellow fluorescent protein (YFP) under the control of the *Cauliflower mosaic virus* (CaMV) 35S promoter was used to transfect tobacco protoplasts. Microscopic analysis showed that the Sl-IAA17–YFP fusion was exclusively localized in the nucleus, in contrast to control protoplasts transformed with YFP alone which displayed fluorescence throughout the cell (**Fig. 1A**).

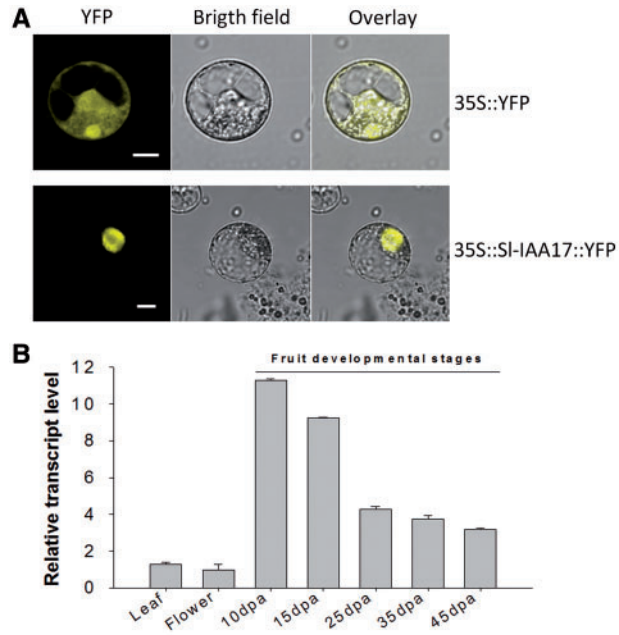


**Fig. 1** Subcellular localization of Sl-IAA17 proteins and profiling of *Sl-IAA17* transcript accumulation in wild-type tomato. (A) Subcellular localization of Sl-IAA17 proteins. Transient transformation in BY-2 tobacco protoplasts showing the nuclear targeting of the Sl-IAA17 protein fused to YFP and expressed under the control of the CaMV 35S promoter. Control cells expressing YFP alone are shown in the top panel. Scale bar = 10 μm. (B) Profiling of *Sl-IAA17* transcript accumulation in wild-type tomato plant tissues monitored by qRT–PCR. The level for flowers was used as a reference. 'F', flower; 'R', root; 'L', leaf; 'dpa', days post-anthesis. The data are mean values corresponding to three independent experiments. Error bars are standard errors.

### *Sl-IAA17* shows high transcript accumulation during tomato fruit development

The analysis of *Sl-IAA17* transcript levels in vegetative and reproductive organs indicated that the expression of *Sl-IAA17* was identical in leaves and flowers (**Fig. 1B**). In contrast, the accumulation of Sl-IAA17 transcripts undergo up to a 10-fold increase in developing fruit when compared with the level in flowers. This dramatic increase in expression starts as early at 10 days post-anthesis (dpa) corresponding to a developmental stage where cell division activities stopped to give way to cell expansion which accounts for fruit growth until ripening (Gillaspy et al. 1993, Joubès et al. 1999). Then, the level of *Sl-IAA17* mRNA declined gradually up to the breaker stage (45 dpa), when the fruit undergoes color change.

### The silencing of *Sl-IAA17* increases tomato fruit size

To gain better insight into the function of Sl-IAA17 in tomato fruit development, we generated RNAi plants and obtained several independent homozygous lines. Three *Sl-IAA17* RNAi lines, named Rline1, Rline2 and Rline3, were selected for further study. The analysis of gene expression by quantitative reverse transcription–PCR (qRT–PCR) showed that the accumulation

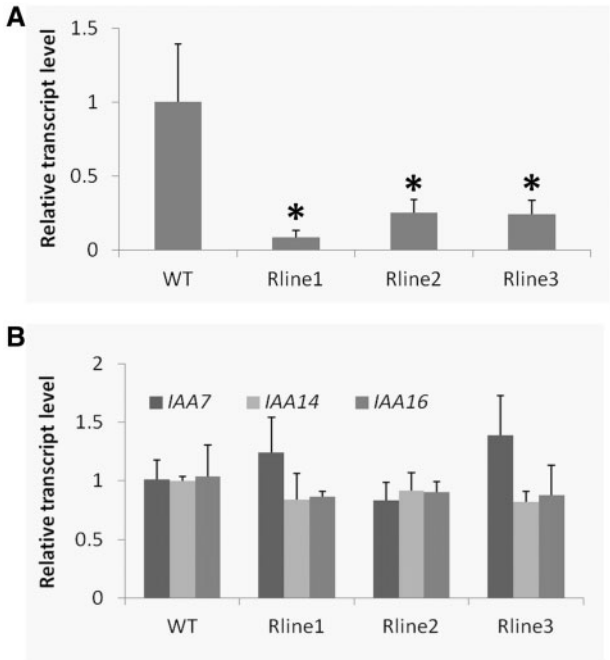


**Fig. 2** Characterization of three independent *Sl-IAA17* RNAi lines. (A) Transcript levels of *Sl-IAA17* in fruit of three independent *Sl-IAA17* RNAi lines (Rline1, Rline2 and Rline3) relative to the wild type (WT), at the 35 dpa stage. Statistical analyses were performed using the *t*-test comparing the WT with each line, $^{*}P < 0.05$. (B) Transcript levels for *Sl-IAA7*, *Sl-IAA14* and *Sl-IAA16* in three independent *Sl-IAA17* RNAi lines (Rline1, Rline2 and Rline3) were assessed in 35 dpa fruit. All the data are mean values corresponding to three independent experiments. Error bars are standard errors.

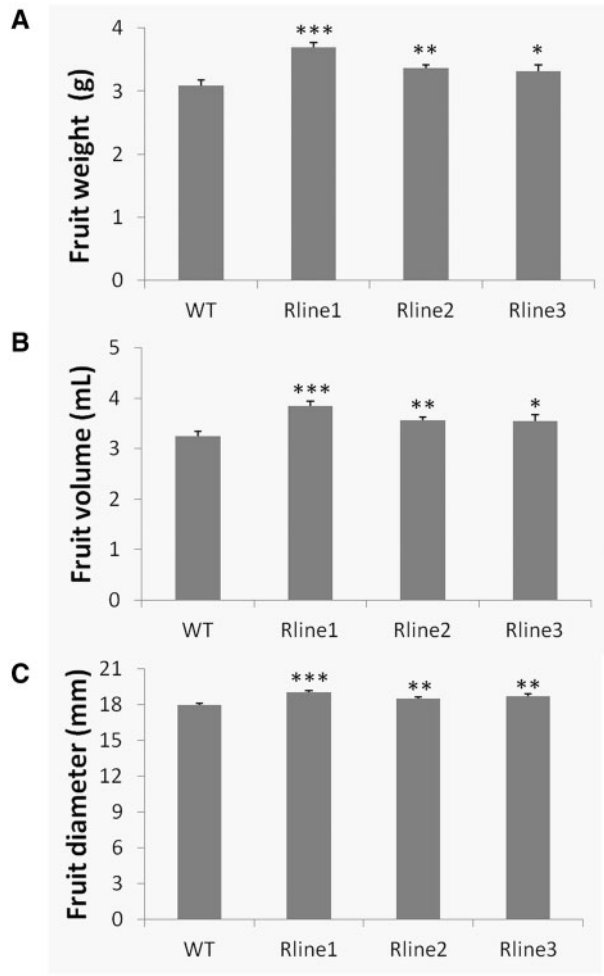


**Fig. 3** Alteration of fruit morphometrical characteristics in *Sl-IAA17* RNAi plants. Fruit weight (A), fruit volume (B) and fruit diameter (C) were determined in fruits harvested at the Br+7 stage (breaker + 7 dpa) from the three independent RNAi plant lines: Rline1, Rline2 and Rline3. The data represent mean values obtained from 50–80 fruits of each line. Statistical analyses were performed using the *t*-test comparing the wild type with each line, $^{***}P < 0.001$; $^{**}P < 0.01$; $^{*}P < 0.05$. Error bars are standard errors.

of *Sl-IAA17* transcripts was strongly reduced in the three RNAi lines when compared with wild-type plants (**Fig. 2A**). Rline 2 and Rline 3 retained 25% of the control mRNA level whereas Rline 1 showed only 9% of the mRNA level displayed in the wild type. To check whether the inhibition by RNAi was specific to *Sl-IAA17*, we assessed the mRNA accumulation of three *Aux/IAA* members, namely *Sl-IAA7*, *Sl-IAA14* and *Sl-IAA16*, belonging to the same clade as *Sl-IAA17*. **Fig. 2B** shows that the RNAi construct did not significantly reduce the mRNA accumulation of these three closelyt homologous genes, even though a slight increase in *Sl-IAA7* transcripts was noticeable in two lines (Rline1 and Rline3) without any statistical significance.

The effects of *Sl-IAA17* silencing on fruit development were then investigated in the three *Sl-IAA17* RNAi lines. An extensivee screening was performed at a late stage of fruit development, namely breaker + 7 d, with the aim of assessing fruit weight, fruit volume, fruit diameter, water content, the number of locules, the number of seeds and other biochemical parameters of ripe fruits. Fruits from *Sl-IAA17* RNAi plants (Rline1, Rline2 and Rline3) displayed a larger size compared with control fruits, weighing up to 19% more than wild-type fruit (**Fig. 3A**). This increase was even more noticeable when measuring the fruit volume (**Fig. 3B**), with RNAi fruit volumes reaching up to 18% more than the wild type. This fruit size enlargement was also observed at the fruit diameter level (**Fig. 3C**), with RNAi fruit displaying up to a 7% average increase in diameter when compared with the wild type. It is noteworthy that the severety of the fruit phenotypic modifications is well correlated with the level of *Sl-IAA17* silencing (**Fig. 2A**), with Rline1 displaying the most pronounced effects. In all tomato RNAi lines tested, the down-regulation of *Sl-IAA17* had no significant effect on the water content (**Supplementary Fig. S4A**). Finally, the locule number and seed number per fruit (**Supplementary Fig. S4B, C**) were similar to those in the wild type, ruling out a possible impact of these tissues on the observed differences in fruit size.

Since the observed differences in fruit size are likely to originate from differences in tissue growth during fruit development, the pericarp and locule thickness (**Fig. 4A**) were measured to investigate further the factors underlying the increase in fruit size and weight encountered in *Sl-IAA17*

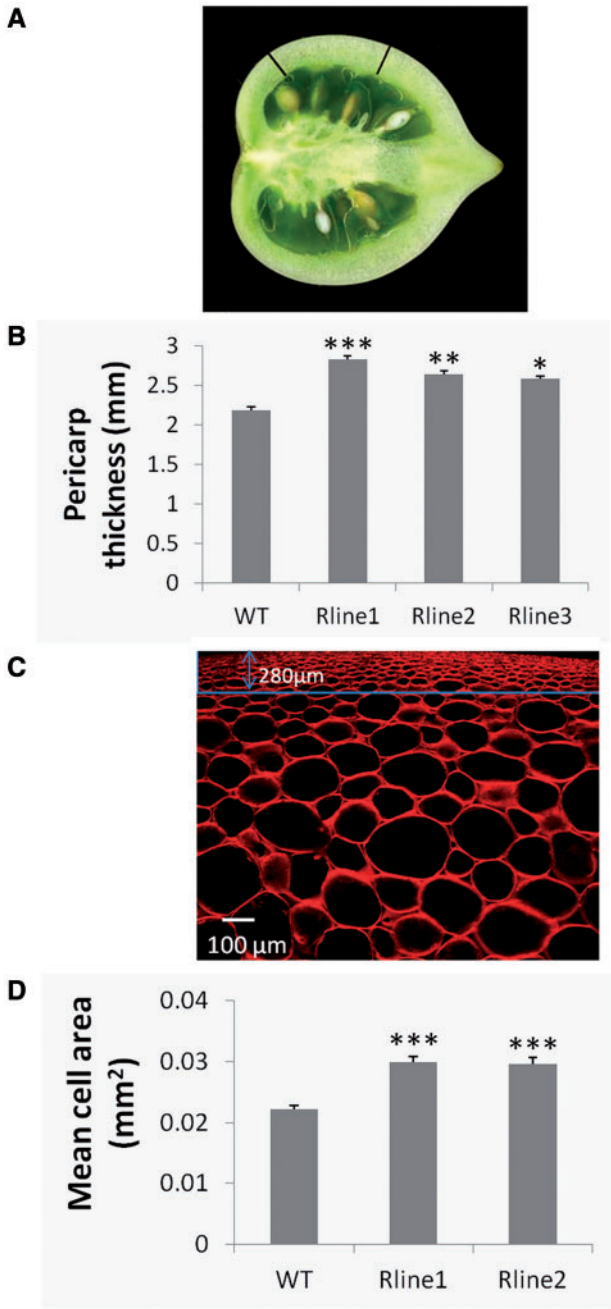


**Fig. 4** Altered thickness and cell size in fruit pericarp in *Sl-IAA17* RNAi tomato lines. (A) The pericarp thickness was measured at the equator of the fruit between the two black lines; these latter were the spots where the microscopic images were taken, as shown in (C) and (D), and between which the tissues were extracted for ploidy analyses. (B) Pericarp thickness of the wild type (WT) and *Sl-IAA17* Rlines. The data represent mean values obtained from 20 fruits at the 35 dpa stage. (C) Confocal image of the pericarp tissue used to measure mean cell area. To take into account the variation of cell size from the skin to the seed locule, the cell number was counted in the same rectangle (represented here), 280 µm away from the first epicuticular cell layer. (D) Tomato pericarp cell mean area of the WT and *Sl-IAA17* Rline1 and Rline2. The data represent mean values obtained from 10 fruits at the 35 dpa stage, two measures per fruit, tissue taken at two different spots on the pericarp, around the black lines shown in (A). Statistical analyses were performed using the *t*-test comparing the WT with each line, *** $P < 0.001$; ** $P < 0.01$; * $P < 0.05$. Error bars are standard errors.

down-regulated lines. Fruits from the three *Sl-IAA17* RNAi lines showed thicker pericarp tissues than the wild type (**Fig. 4B**). This difference reached up to 28% in Rline1, where the *Sl-IAA17* transcript accumulation was the most reduced (**Fig. 2A**). However, there was no significant differences in the locule thickness between all the three lines (data not shown).

## The down-regulation of *Sl-IAA17* increases the pericarp cell size and nuclear ploidy levels

In order to analyze the pericarp at the cellular level, microscopic observations were performed, showing that the cells in the pericarp of the RNAi lines were much larger than those in the wild type (**Fig. 4C**, **D**). This increase in mean cell size reached up to a 36% difference. In the same set of microscopic observations, we did not notice any significant differences in the number of pericarp cell layers using fruits either at the immature green stage (25 dpa) or at the mature green stage (35 dpa) (**Supplementary Fig. S4**). Hence the differences in pericarp thickness observed in the RNAi lines are due to enhanced cell size rather than increased cell number.

Since a correlation exists between cell size and the nuclear DNA ploidy level resulting from endoreduplication in tomato fruit (Cheniclet et al. 2005, Chevalier et al. 2011, Bourdon et al. 2012, Chevalier et al. 2014), we checked whether such a relationship existed between the increase in pericarp cell size in the RNAi *Sl-IAA17* transgenic fruit and the endoreduplication level of these cells. The nuclear DNA content (ploidy level) of pericarp cells from wild-type and the three independent *Sl-IAA17* RNAi fruits, harvested at 35 dpa, was determined by flow cytometry (**Fig. 5**). The analysis revealed that the nuclear DNA ploidy level of the pericarp cells from the three transgenic lines increased significantly: the mean ploidy level of the transgenic fruits was about 20% higher than that in wild-type fruit (**Fig. 5A**). The endoreduplication index (EI) was significantly increased in Rline1 (2.42), Rline2 (2.47) and Rline3 (2.33) when compared with that in wild type (2.19). Furthermore, the nuclear DNA ploidy distribution in the three RNAi lines showed increases mostly for the 32C and 64C peaks and also in some cases for the 128C peak compared with the wild type, suggesting the promotion of successive endocycles in transgenic *Sl-IAA17* RNAi lines (**Fig. 5B**). For the most affected lines, Rline1 and Rline2, there was a decrease for the 2C and 4C DNA levels compared with the wild type. These data show that the cell expansion in the down-regulated *Sl-IAA17* transgenic fruits is tightly coupled to the level of endoreduplication and suggest that Sl-IAA17 could be involved in the control of endoreduplication in tomato fruits.

## Discussion

After successful flower pollination and ovule fertilization, fruit and seed initiation (during so-called fruit set) and subsequent development occur concomitantly according to a tightly genetically controlled process operated by phytohormones (Gillaspy et al. 1993). In the early fruit developmental stages, plant hormones exert a direct control on cell division and cell

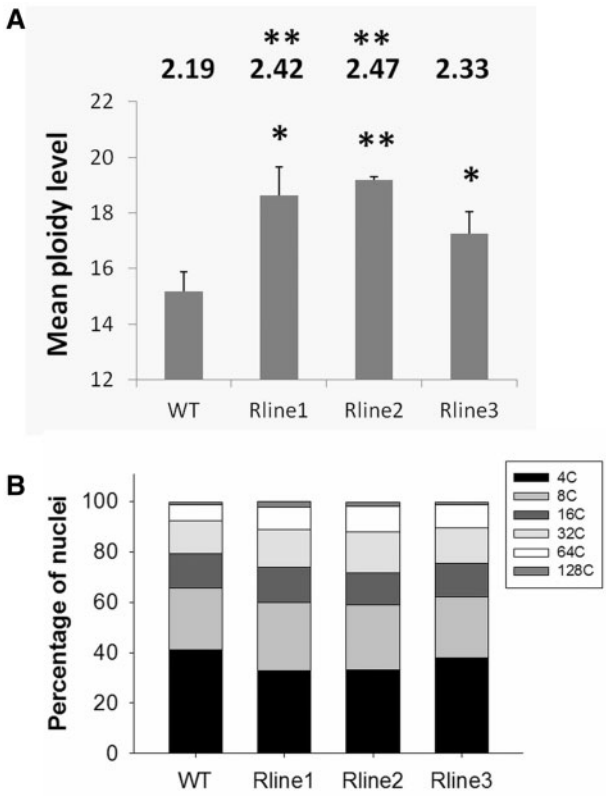


**Fig. 5** Altered ploidy level in fruit pericarp cells of *Sl-IAA17* RNAi tomato lines. (A) Effect of *Sl-IAA17* RNAi transformation on the mean ploidy level in tomato fruit at the 35 dpa stage. Endoreduplication index (EI) values are indicated above each bar of the histogram. (B) Proportion of each ploidy level of the wild type (WT) and three RNAi lines. Ploidy was analyzed by flow cytometry in the pericarp of five fruits of each line, with tissue taken within the two black lines as shown in **Fig. 4A**. Statistical analyses were performed using the *t*-test comparing the WT with each line, $^{**}P < 0.01$; $^{*}P < 0.05$. Error bars are standard errors.

expansion processes that determine the cell number and cell size, respectively, inside tomato fruit (Gillaspy et al. 1993, Ruan et al. 2012, Ariizumi et al. 2013, Pattison et al. 2014). As a result, the combination of cell number and cell size drives fruit growth, and influences the final fruit size.

In the present study, we describe a functional analysis of *Sl-IAA17* encoding a member of the tomato *Aux/IAA* gene family. At the level of its primary sequence, Sl-IAA17 displays all the characteristics of an Aux/IAA transcriptional repressor, in particular the presence of the canonical repressor domain I (Tiwari et al. 2004) and a putative second repressor domain of the DLxLxL type. The presence of these domains is in agreement with our previous demonstration that the Sl-IAA17 protein functions as an active repressor of auxin-dependent gene transcription (Audran-Delalande et al. 2012). In addition, the exclusive subcellular localization of Sl-IAA17 within the nucleus (**Fig. 1A**) is fully consistent with a transcriptional regulatory function.

The expression profile of *Sl-IAA17* revealed a preferential accumulation of transcripts in the early developing fruit, with a maximum expression at 10 dpa (**Fig. 1B**). Interestingly, mining RNaseq data available for the development of tomato in the Heinz cultivar also revealed a strong up-regulation of *Sl-IAA17* after pollination within the developing fruits, and then a decline in expression at the mature green stage (http://ted.bti.cornell.edu/; **Supplementary Fig. S2**). These observations thus suggest a putative role for *Sl-IAA17* in early fruit development, as previously observed for other *Sl-IAA* genes (Wang et al. 2005, Wang et al. 2009, Bassa et al. 2012). Classically, a bimodal pattern of auxin flux during tomato fruit development is described in the literature (Gillaspy et al. 1993, Srivastava and Handa, 2005): a first peak in activity occurs at about 10 dpa and then a second one at about 30 dpa in developing tomato fruits, which thus suggests that auxin controls the initiation of the cell expansion phase (phase III) and initiation of the ripening process and final embryo development phase (phase IV), corresponding, respectively, to these two developmental time points. Remarkably, the peak of *Sl-IAA17* expression coincides with the first peak of auxin concentration at 10 dpa, associated with the promotion of cell elongation and thus accelerated fruit expansion (Pattison et al. 2014).

Down-regulating *Sl-IAA17* in tomato transgenic plants resulted in an increased fruit size (**Fig. 3**). The phenotypic analysis of fruits from the three generated RNAi lines revealed that this increase in fruit size was associated with a thicker pericarp, resulting from an enhanced cell expansion and not from a higher number of cells (**Fig. 4**; **Supplementary Fig. S4**). The effect on fruit growth is likely to be specific for the down-regulation of *Sl-IAA17*, since the expression of other *Aux/IAA* genes belonging to the same supposed functional clade is unaffected in the three RNAi lines (**Fig. 2**). It is known that the number of locules greatly influences the final fruit size (Tanksley 2004), and that seeds promote fruit expansion through producing or delivering auxins to the surrounding tissues (Ariizumi et al. 2013, and references therein). In our observations, the effect on fruit size is only related to modifications within the pericarp and did not originate from a higher number of locules or seeds (**Supplementary Fig. S3**).

In various plant cell types, a correlation has often been found between cell size and the nuclear DNA ploidy level resulting from the endoreduplication process (Joubés and Chevalier 2000, Sugimoto-Shirasu and Roberts 2003, Inze and De Veylder 2006). Hence we could clearly demonstrate that down-regulating *Sl-IAA17* in tomato transgenic plants promotes endoreduplication inside the pericarp cells which enhances cell expansion (**Fig. 5**), thus resulting in the increase of fruit size. In tomato, endoreduplication plays a functional role in regulating the karyoplasmic homeostasy during fruit development (Chevalier et al. 2011, Bourdon et al. 2012, Chevalier et al. 2014), and fruit size is largely dependent upon the endoreduplication-associated cell expansion inside the pericarp tissue (Cheniclet et al. 2005). Not only are these data in full agreement with the influence of endoreduplication on cell expansion and consequently on fruit growth/size, but they reveal an active role for auxin signaling in the transition from the mitotic cycle to the endocycle in tomato fruit cells. It has been reported that auxin modulates the switch from mitotic

cycles to the endocycle in the root meristem in Arabidopsis (Ishida et al. 2010). Furthermore, it was suggested that the mitotic to endocycle transition is mediated by the TIR1–AUX/IAA–ARF-dependent auxin signaling pathway. However, in contrast to the situation in Arabidopsis root meristem tissues where the ploidy distribution was significantly increased as a result of gain-of-function mutations in *IAA7/AXR2* and *IAA17/AXR3* genes, the effect of *Sl-IAA17* down-regulation reported herein seems to lead to a higher nuclear DNA ploidy level in tomato fruits. These seemingly contradictory data may be resolved by the different nature of the tissues and development processes involved, namely the fruit organ in tomato and the root tissue in Arabidopsis. Moreover, since ARF proteins, the natural partners of Aux/IAAs, can act either as repressors or as activators of gene transcription, it cannot be ruled out that Sl-IAA17 may interact with different ARFs in the different tissues, leading to transcriptional repression of target genes in one case and to transcriptional activation in the other case.

In conclusion, our data demonstrate that the repression of Sl-IAA17 affects the size of fruit pericarp cells, via an increase in the ploidy levels, which ultimately influences the final size of the fruit. This suggests that auxin signaling contributes to controlling the onset of endoreduplication; however, further functional studies are required to investigate the molecular mechanisms by which Sl-IAA17 and auxin signaling may control endoreduplication. The Sl-IAA17 RNAi fruit series generated in this study now offer a suitable tool to better unravel these mechanisms and the associated gene network, while bearing in mind that the endocycle is under the control of several key components (Chevalier et al. 2011).

## Materials and Methods

### Plant material and growth conditions

Tomato seeds (*Solanum lycopersicum* cv. MicroTom) were sterilized for 5 min in bleach, rinsed in sterile water and sown in recipient Magenta vessels containing 50 ml of 50% Murashige and Skoog (MS) culture medium and 0.8% (w/v) agar, pH 5.9. Plants were grown in culture rooms as follows: 14 h/10 h day/night cycle; 25/20°C day/night temperature; 80% relative humidity; 250 μmol $m^{-2}$ $s^{-1}$ light intensity. The number of fruits per plant was restricted to 12, i.e. three bunches of four fruit, left after fertilization, in order to limit the fruit size variability due to the variability in the number of fruit per plant.

### Sequence data and analysis

Sequence data for the Arabidopsis genes used in this article can be found in the Arabidopsis Genome Initiative data library under the following accession numbers: *AtIAA17* (AT1G04250), *AtIAA7* (AT3G23050), *AtIAA14* (AT4G14550) and *AtIAA16* (AT3G04730).

Sequence data for the tomato genes used in this article can be found in the GenBank/EMBL data libraries under the following accession numbers: *Sl-IAA17* (JN379444), *Sl-IAA7* (JN379435), *Sl-IAA14* (JN379441) and *Sl-IAA16* (JN379443).

### Transient expression using a single-cell system

For nuclear localization of the Sl-IAA17 protein, the *Sl-IAA17* open reading frame was cloned by Gateway technology (using the combination of 5′AAAAAGCAGGCTTCATGAGTAGTAATAAGTTG3′ forward and 5′AGAAAGCTGGGTGTCATCCATTTCTGTTC3′ reverse primers) in-frame with YFP into the pEarlyGate104 vector, and expressed under the control of the 35S CaMV promoter. The empty vector pEarlyGate104 was used as a control. Protoplasts were obtained from suspension-cultured tobacco (*Nicotiana tabacum*) BY-2 cells, transfected according to the method described previously, and YFP localization was monitored using confocal microscopy as described previously (Audran-Delalande et al. 2012).

### Plant transformation

The forward primer P1 (5′AAAAAGCAGGCTTCATGAGTAGTAATAAGTTG3′) and reverse primer P2 (5′AGAAAGCTGGGTGCCTTGGCAGCTGGGGTTTTGTGTG 3′) were used to amplify a 196 bp long *Sl-IAA17* sequence, with annealing temperature set at 55°C. This fragment was cloned into the pDonr207 vector and then into the pHellsgate12 vector using Gateway technology (Invitrogen). RNAi transgenic plants were generated via *Agrobacterium tumefaciens*-mediated transformation according to Wang et al. (2005). All experiments were carried out using homozygous lines from $F_3$ or later generations.

### RNA extraction and gene expression analysis by qRT–PCR

Total RNA was extracted using a Plant RNeasy Mini kit (Qiagen, http://www.qiagen.com) according to the manufacturer's instructions. Total RNA was treated by DNase I to remove any genomic DNA contamination. First-strand cDNA was reverse transcribed from 2 μg of total RNA using the Omniscript kit (Qiagen) according to the manufacturer's instructions. qRT–PCR analyses were performed as described previously (Chervin and Deluc 2010). Gene-specific primers were designed using the Primer Express 1.0 software (PE-Applied Bio-systems). The sequences of primers used in this study are listed in **Supplementary Table S1**. Actin was used as an internal control.

### Tomato fruit phenotyping and pericarp thickness analyses

Eighty fruits from 24 different plants were chosen for each line at the breaker + 7 d stage (about 45 dpa), and assessed for various fruit quality traits such as weight, volume (assessed by measuring the water displacement in a small measuring cylinder after plunging the fruit in), diameter (assessed with a Harpenden Skinfold Caliper), number of locules, number of seeds and water content (assessed by measuring weight loss of a fruit section after dessication for 3 d at 60°C). For pericarp thickness, a different culture was used: 20 fruits at the mature green stage (35 dpa) of an average volume (as shown in **Fig. 3B**) were selected for each tomato line. Fruits at the mature green stage have almost reached their final size, but pericarp cells are more rigid than in red ripe fruits, giving less variable readings. Vertical sections of each fruit were scanned; pericarp thickness measurements were performed at the equator of the fruit somewhere between the two black lines as shown in **Fig. 4A**, and the images were analyzed using ImageJ software.

### Cytological analyses

Ten fruits at the mature green stage for each line were selected. Thin pericarp slices (80 μm thick) were cut using a vibratome (Vibratome LEICA VT 1000S), stained with Congo red for 2 min at room temperature, then rinsed briefly in water immediately before observation. Images were acquired by confocal laser scanning microscopy (TCS SP2 AOBS; Leica Instruments) using a ×10 dry objective lens (numerical aperture 0.30; PL FLUOTAR). Fluorescence emission spectra were acquired using the 561 nm wavelength of a laser diode and recorded in one of the confocal channels in the 569–662 nm emission range. Images were acquired using Leica LCS software (version 2.61). For each fruit, two zones of the pericarp were analyzed around each black line, as shown in **Fig. 4A**. To assess the number of cell layers from the outer epidermis to the limit of the locule, a straight line was drawn in the middle of each image (an image sample is shown in **Fig. 4C**), and the number of cells intersecting this line was counted. The mean pericarp cell size was estimated using the following method: in each image, we counted the number of cells appearing within a rectangle, as shown in **Fig. 4C** (width × height = 1,500 × 1,220 μm), the top of which was parallel to the outer epidermis, but 280 μm below the first outer epidermis cell layer, in order to avoid counting the small cells which create lots of variability and error. The average cell area (in $mm^2$) was calculated from the ratio 1.5 × 1.22/number of cells.

## Ploidy analyses

Nuclei were prepared from pericarp tissues of five fruits at the mature green stage of an average weight for the wild-type line and the three *Sl-IAA17* down-regulation lines (Rline1, Rline2 and Rline3). The pericarp tissues (0.1–0.2 g FW) were chopped with a razor blade in 0.5 ml of Partec suspension solution, then 0.7 ml of Cystain UV ploidy solution (Partec) was added. The suspension was filtered through a 100 μm nylon mesh. The combined filtrates were analyzed using the CyFlow® Space flow cytometer from Partec. Ploidy histograms were quantitatively analyzed using the DPAC software (Partec), after manual treatment to exclude noise. The mean ploidy level of each pericarp tissue was calculated as the sum of each C value class weighed by its frequency. The EI was calculated according to Barow and Meister (2003).

## Supplementary data

**Supplementary data** are available at PCP online.

## Funding

This work was supported by the French Laboratory of Excellence [project 'TULIP' (ANR-10-LABX-41; ANR-11-IDEX-0002-02)]. This work benefited from the networking activities within the European funded COST ACTION FA1106 'Qualityfruit'. Liyan Su was supported by the China Scholarship Council, Carole Bassa was supported by the Ministère de la Recherche et de l'Enseignement Supérieur.

## Acknowledgments

We are grateful to the staff of the Cellular Imaging Facility of 'Fédération de Recherche FR3450 Castatnet-Tolosan' (FRAIB, TRI Platform) for microscopy analyses and to the GeT-PlaGe staff for maintenance of the qPCR equipement (GenoToul Platform). We thank O. Berseille, L. Lemonnier and D. Saint-Martin (UMR990 GBF) for generation of transgenic lines and tomato culture.

## Disclosures

The authors have no conflicts of interest to declare.

## References

Ariizumi, T., Shinozaki, Y. and Ezura, H. (2013) Genes that influence yield in tomato. *Breed. Sci.* 63: 3–13.

Audran-Delalande, C., Bassa, C., Mila, I., Regad, F., Zouine, M. and Bouzayen, M. (2012) Genome-wide identification, functional analysis and expression profiling of the Aux/IAA gene family in tomato. *Plant Cell Physiol.* 53: 659–672.

Bargman, B.O.R. and Estelle, M. (2014) Auxin perception: in the IAA of the beholder. *Physiol. Plant.* 151: 52–61.

Barow, M. and Meister, A. (2003) Endopolyploidy in seed plants is differently correlated to systematics, organ, life strategy and genome size. *Plant Cell Environment.* 26: 571–584.

Bassa, C., Mila, I., Bouzayen, M. and Audran-Delalande, C. (2012) Phenotypes associated with down-regulation of Sl-IAA27 support functional diversity among Aux/IAA family members in tomato. *Plant Cell Physiol.* 53: 1583–1595.

Bourdon, M., Pirrello, J., Cheniclet, C., Coriton, O., Bourge, M., Brown, S. et al. (2012) Evidence for karyoplasmic homeostasis during endoreduplication and a ploidy-dependent increase in gene transcription during tomato fruit growth. *Development* 139: 3817–3826.

Cheniclet, C., Rong, WY., Causse, M., Frangne, N., Bolling, L., Cardeet, J.P. et al. (2005) Cell expansion and endoreduplication show a large genetic variability in pericarp and contribute strongly to tomato fruit growth. *Plant Physiol.* 139: 1984–1994.

Chervin, C. and Deluc, L. (2010) Ethylene signalling receptors and transcription factors over the grape berry development: gene expression profiling. *Vitis* 49: 129–136.

Chevalier, C.E., Bourdon, M., Frangne, N., Cheniclet, C. and Gévaudant, F. (2014) Endoreduplication and fruit growth in tomato: evidence in favour of the karyoplasmic ratio theory. *J. Exp. Bot.* 65: 2731–2746.

Chevalier, C., Nafati, M., Mathieu-Rivet, E., Bourdon, M., Frangne, N., Cheniclet, C. et al. (2011) Elucidating the functional role of endoreduplication in tomato fruit development. *Ann. Bot.* 107: 1159–1169.

De Jong, M., Wolters-Arts, M., Feron, R., Mariani, C. and Vriezen, W.H. (2009) The Solanum lycopersicum auxin response factor 7 (SlARF7) regulates auxin signalling during tomato fruit set and development. *Plant J.* 57: 160–170.

Devoghalaere, F., Doucen, T., Guitton, B., Keeling, J., Payne, W., Ling, T.J. et al. (2012) A genomics approach to understanding the role of auxin in apple (Malus×domestica) fruit size control. *BMC Plant Biol.* 12: 7.

Dharmasiri, N., Dharmasiri, S., Weijers, D., Lechner, E., Yamada, M., Hobbie, L. et al. (2005) Plant development is regulated by a family of auxin receptor F box proteins. *Dev. Cell* 9: 109–119.

Gillaspy, G., Ben-David, H. and Gruissem, W. (1993) Fruits: a developmental perspective. *Plant Cell* 5: 1439–1451.

Goetz, M., Vivian-Smith, A., Johnson, S.D. and Koltunow, A.M. (2006) AUXIN RESPONSE FACTOR8 is a negative regulator of fruit initiation in Arabidopsis. *Plant Cell* 18: 1873–1886.

Hao, Y., Wang, X., Li, X., Bassa, C., Mila, I., Audran-Delalande, C. et al. (2014) Genome-wide identification, phylogenetic analysis, expression profiling and protein–protein interaction properties of the *Topless* gene family members in tomato. *J. Exp. Bot.* 65: 1013–1023.

Inze, D. and De Veylder, L. (2006) Cell cycle regulation in plant development. *Annu. Rev. Genet.* 40: 77–105.

Ishida, T., Adachi, S., Yoshimura, K., Shimizu, K., Umeda, M. and Sugimoto, K. (2010) Auxin modulates the transition from mitotic cycle to the endocycles in Arabidopsis. *Development* 137: 63–71.

Joubés, J. and Chevalier, C. (2000) Endoreduplication in higher plants. *Plant Mol. Biol.* 43: 737–747.

Joubès, J., Phan, T.H., Just, D., Rothan, C., Bergounioux, C., Raymond, P. et al. (1999) Molecular and biochemical characterization of the involvement of cyclin-dependent kinase CDKA during the early development of tomato fruit. *Plant Physiol.* 121: 857–869.

Kepinski, S. and Leyser, O. (2005) The Arabidopsis F-box protein TIR1 is an auxin receptor. *Nature* 435: 446–451.

Kloosterman, B., Visser, R.G.F. and Bachem, C.W.B. (2006) Isolation and characterization of a novel potato Auxin/Indole-3-Acetic Acid family member (StIAA2) that is involved in petiole hyponasty and shoot morphogenesis. *Plant Physiol. Biochem.* 44: 766–775.

Ljung, K. (2013) Auxin metabolism and homeostasis during plant development. *Development* 140: 943–950.

Pattison, R.J., Csukasi, F. and Catala, C. (2014) Mechanisms regulating auxin action during fruit development. *Physiol. Plant.* 151: 62–72.

Rinaldi, M.A., Liu, J., Enders, T.A., Bartel, B. and Strader, L.C. (2012) A gain-of-function mutation in IAA16 confers reduced responses to auxin and abscisic acid and impedes plant growth and fertility. *Plant Mol. Biol.* 79: 359–373.

Ruan, Y.L., Patrick, J.W., Bouzayen, M., Osorio, S. and Fernie, A.R. (2012) Molecular regulation of seed and fruit set. *Trends Plant Sci.* 17: 656–665.

Sagar, M., Chervin, C., Mila, I., Hao, Y., Roustan, J.P., Benichou, M. et al. (2013) SlARF4, an auxin response factor involved in the control of sugar

metabolism during tomato fruit development. *Plant Physiol.* 161: 1362–1374.

Srivastava, A. and Handa, A.K. (2005) Hormonal regulation of tomato fruit development: a molecular perspective. *J. Plant Growth Regul.* 24: 67–82.

Sugimoto-Shirasu, K. and Roberts, K. (2003) 'Big it up': endoreduplication and cell-size control in plants. *Curr. Opin. Plant Biol.* 6: 544–553.

Tanksley, S.D. (2004) The genetic, developmental, and molecular bases of fruit size and shape variation in tomato. *Plant Cell* 16: S181–S189.

Tiwari, S.B., Hagen, G. and Guilfoyle, T.J. (2004) Aux/IAA proteins contain a potent transcriptional repression domain. *Amer. Soc. Plant Biol.* 16: 2533–2543.

Tomato Genome Consortium. (2012) The tomato genome sequence provides insights into fleshy fruit evolution. *Nature* 485: 635–641.

Wang, H., Jones, B., Li, Z., Frasse, P., Delalande, C., Regad, F. et al. (2005) The tomato Aux/IAA transcription factor IAA9 is involved in fruit development and leaf morphogenesis. *Plant Cell* 17: 2676–2692.

Wang, H., Schauer, N., Usadel, B., Frasse, P., Zouine, M., Hernould, M. et al. (2009) Regulatory features underlying pollination-dependent and independent tomato fruit set revealed by transcript and primary metabolite profiling. *Plant Cell* 21: 1428–1452.

Zouine, M., Fu, Y., Chateigner-Boutin, A.L., Mila, I., Wang, H., Audran, C. et al. (2014) Characterization of the tomato *ARF* gene family uncovers a multi-levels post-transcriptional regulation including alternative splicing. *PLoS One* 9: e84203.